

Corrosion Evaluation of Steels Under Geothermal CO₂ Supercritical Conditions

Francois Ropital and Jean Kittel

IFP Energies nouvelles, Rond-point de l'échangeur de Solaize, BP 3, 69360 Solaize, France

francois.ropital@ifpen.fr, jean.kittel@ifpen.fr

Keywords: corrosion, steels, carbon dioxide, supercritical

ABSTRACT

Corrosion is one of the major issues in the development of high enthalpy geothermal systems. In some fields, the CO₂ pressure and the temperature are respectively greater than 77 bar and 31°C, and the supercritical conditions of CO₂ can lead to severe corrosion damages for carbon and stainless steel geothermal equipment. If supercritical CO₂ can occur naturally in a reservoir, it is also a promising heat transmission fluid for enhanced geothermal systems (EGS). The quantity of water associated with the supercritical CO₂ is also an important parameter. In order to study these effects, experimental tests have been performed in autoclaves in both supercritical CO₂ and water phases. Carbon steels and several stainless steels grades (AISI 410, 304L, 316L, 2205 duplex, 2507 duplex, 254 SMO) have been tested at 110°C under 160 bar of CO₂ and different water compositions and with CO₂ contamination by oxygen. Carbon steel coupons and AISI 410 stainless steel suffer uniform corrosion damages and the other stainless steel grades have more localized degradation for the oxygen contamination conditions.

1. INTRODUCTION

Supercritical geothermal systems are located at near or below depths of the brittle-ductile transition zone in the Earth's crust where the reservoir fluid is assumed to be in the supercritical state, for example above 374 °C and 221 bar for pure water, or above 77 bar and 31°C for pure CO₂. These systems are unconventional geothermal resources with high productivity due to their high enthalpy fluids. The work of the corrosion literature mainly concerns the vapor phase fluids leaving the supercritical conditions. The corrosive elements in the vapor phase may be H₂S (high temperature sulfidation) but also HCl, HF and NH₃ (Truesdell AH et al., 1989) (Cabrini M et al., 2017) (Kruszeski and Witting 2018). In addition, if supercritical CO₂ can occur naturally in a reservoir, it is also a promising heat transmission fluid for enhanced geothermal systems (EGS). It is well recognized that dry supercritical (sc) CO₂ is not corrosive for carbon and stainless steel (Zhang et al. 2013). For wet sc CO₂ systems, information on the corrosion in the sc CO₂ and water phases is more limited: the corrosion rate can depend on the humidity of sc CO₂ (Hua et al. 2015). Most of the laboratory experiments have been performed under moderate conditions, up to 50°C, 100 bar and for short time periods (Brown et al. 2014). Some attack of the passive layer of low grade stainless steels such as AISI 310 and localized corrosion may be suspected (Zhang et al. 2013). In order to get a better knowledge of the water composition effect and the oxygen contamination, experimental work was performed on two grades of carbon steel and six grades of corrosion resistant steel (AISI 410, 304L, 316L, 2205 duplex, 2507 duplex, 254 SMO) at 110°C under 160 bar of CO₂ pressure.

2. EXPERIMENTAL CONDITIONS

2.1 Autoclave tests conditions

The corrosion tests were performed in a 16L Hastelloy C276 autoclave. All the experiments were performed in supercritical CO₂ conditions at 110°C under 160 bar of CO₂ pressure. Four liters of water were introduced in the autoclave. Two phases were present and neither the water nor the CO₂ were replaced during the experiment. The solution and the autoclave were deaerated by nitrogen bubbling. Weight loss corrosion coupons were placed in the water and sc CO₂ phases of the corrosion media. The main corrosion parameters were the salinity of the water and the contamination of carbon dioxide with oxygen. The three test conditions are presented in Table 1.

Table 1: Corrosion tests conditions

	Solution	T (°C)	P CO ₂ (bar)	% oxygen in CO ₂
Test 1	Pure water	110	160	0
Test 2	Water with 50 g/L NaCl	110	160	0
Test 3	Water with 50 g/L NaCl	110	160	2

2.2 Materials

Two carbon steels (AISI 1018 and A516 grade 60) and six stainless steel grades (ferritic AISI 410, austenitic 304L, austenitic 316L, duplex 2205, duplex 2507, austenitic 254 SMO) were evaluated. The carbon steel and stainless steel compositions are respectively indicated in Table 2 and 3. The samples were purchased from Metal Samples and their size is 76.2 x 12.7 x 1.6 mm (except for AISI 410 coupons which size is 27 x 27 x 1.5 mm).

Table 2: Composition of the carbon steels coupons (weight %)

	% C	% Mn	% Si	% P	% Si
AISI 1018	0.18	0.84	0.02	0.010	0.005
A516 grade 60	0.17	0.95	0.21	0.015	0.011

Table 3: Composition of the stainless steels coupons (weight %)

	% C	% Cr	% Ni	% Mo	% Si	% N
AISI 410	0.13	11.85	0.27		0.42	
AISI 304L	0.028	17.7	8.1		0.27	0.09
AISI 316L	0.020	16.9	10.3	2.16	0.416	0.047
2205	0.016	22.3	5.71	3.21	0.38	0.174
2507	0.017	25.5	7.1	3.86	0.20	0.282
254 SMO	0.011	20.0	18.0	6.07	0.27	0.198

2.3 Methodology of evaluation of the corrosion

Before the experiments the sizes of the samples were measured, then the samples were degreased and weighted. After the tests, pictures of the samples were taken and their weight measured before and after cleaning according to ASTM G1 protocol. The corrosion rates were then determined.

3 CORROSION TESTS RESULTS

3.1 Influence of the water composition

The corrosion rates measured after 30 days are reported in Table 4.

For test 1 (pure water) and test 2 (50g/L NaCl), no corrosion attacks were observed for the austenitic 304L, austenitic 316L, duplex 2205, duplex 2507 and, austenitic 254 SMO stainless steel.

Uniform corrosion damages appeared on the two carbon steel steels located in the sc CO₂ phase (Figure 1): for the two waters composition, the general corrosion rate was low ($\approx 10 \mu\text{m}/\text{year}$). In the sc CO₂ phase, a slight attack was noticed for the AISI 310 coupons.

The uniform corrosion rates were much higher for the coupons located in the water phase (Figure 2) even for the AISI 310 stainless steel for which the corrosion rate was around 0.25 mm/year in water containing 50 g/L NaCl due to a general attack of the passive layer. The increase of the water salinity increased the uniform corrosion rate in the water phase.

Table 4: Corrosion rates with Test 1 and 2 conditions

	Test 1 (Pure water) sc CO ₂ phase ($\mu\text{m}/\text{year}$)	Test 1 (Pure water) water phase ($\mu\text{m}/\text{year}$)	Test 2 (50 g/L NaCl) sc CO ₂ phase ($\mu\text{m}/\text{year}$)	Test 2 (50 g/L NaCl) water phase ($\mu\text{m}/\text{year}$)
AISI 1810	15 \pm 5	110 \pm 20	10 \pm 5	550 \pm 50
A516 grade 60	8 \pm 5	70 \pm 20	12 \pm 5	235 \pm 30
AISI 310	3 \pm 2	64 \pm 20	2 \pm 1	245 \pm 30

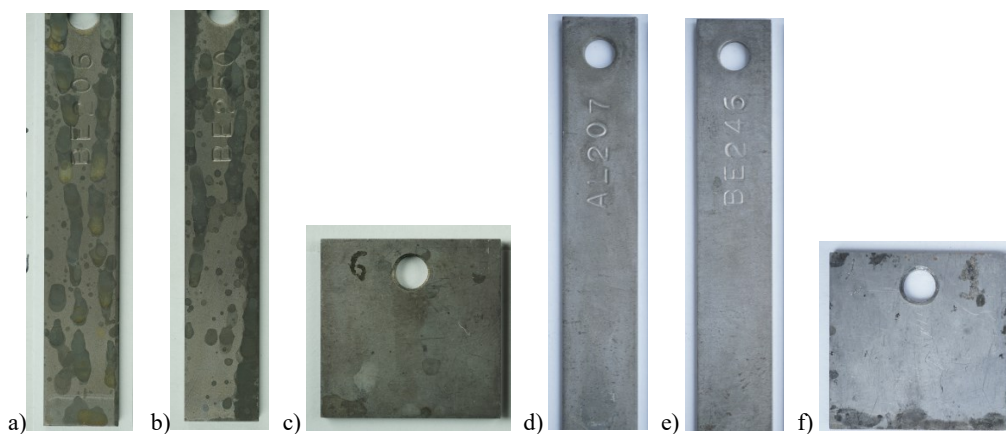


Figure 1: Samples after 30 days in the sc CO₂ phase of Test 1 (pure water) after cleaning a) 1018 carbon steel b) A516 carbon steel c) AISI 310 stainless steel and in the sc CO₂ phase of Test 2 d) 1018 carbon steel e) A516 carbon steel f) AISI 310 stainless steel

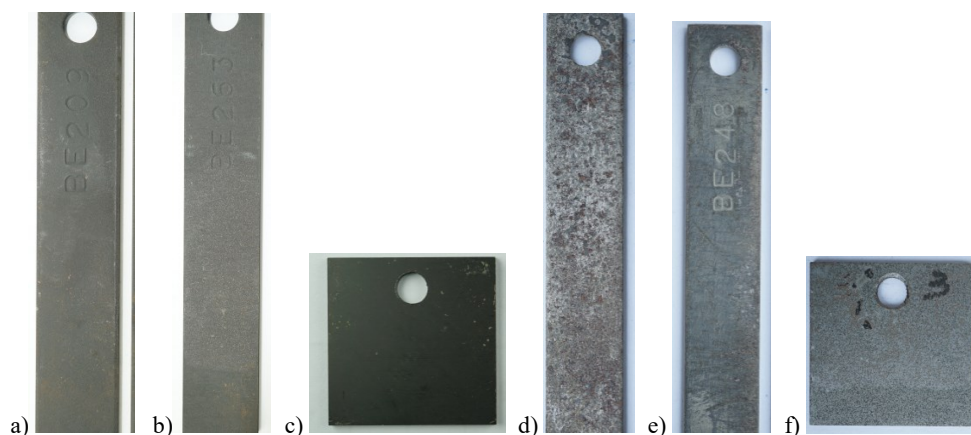


Figure 2: Samples after 30 days in the water phase of Test 1 (pure water) after cleaning a) 1018 carbon steel b) A516 carbon steel c) AISI 410 stainless steel and in the water phase of Test 2 d) 1018 carbon steel e) A516 carbon steel f) AISI 410 stainless steel

3.2 Influence of oxygen contamination in CO₂

The impact of a 2% oxygen contamination of the CO₂ was evaluated in the 50 g/L sodium chloride solution. All the samples were immersed in the water phase. The test was stopped after 6 days due to a leak of the gas supply line, which appeared to be caused by internal corrosion. The corrosion results are presented in Table 5.

**Table 5: Corrosion rates with Test 3 conditions (2% O₂ in CO₂, 50 g/L NaCl solution)
(- few pits , +++ many pits and crevices)**

	AISI 1018	A516 Gr60	AISI 410	AISI 304L	AISI 316L	2205	2507	254 SMO
Corrosion type	Uniform	Uniform	Uniform	Localized +++	Localized +++	Localized ++	Localized +	Localized -
Corrosion rate (mm/year)	5.5 ± 1	6.2 ± 1	4.0 ± 1					

Figure 3 shows the uniform attack of the carbon steel and the AISI 410 stainless steel coupons. The AISI 410 ferritic stainless suffered severe depassivation.

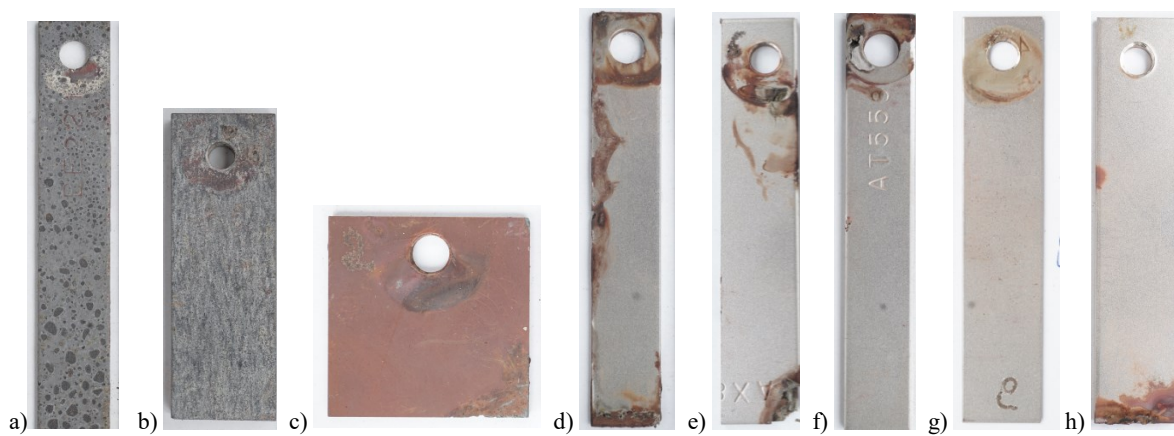


Figure 3: Samples after 6 days in the water phase of Test 3 before cleaning a) 1018 carbon steel b) A516 carbon steel c) AISI 410 stainless steel d) 304L stainless steel e) 316L stainless steel g) 2205 stainless steel g) 2507 stainless steel h) 254 SMO stainless steel

Localized attacks of austenitic 304L, austenitic 316L, duplex 2205, duplex 2507 and super austenitic 254 SMO samples can be noticed on Figure 3. The more resistant stainless is the super austenitic 254 SMO that contains 6% molybdenum. In order to get a better corrosion resistance when oxygen is dissolved, nickel or titanium alloys should be preferred.

CONCLUSION

This work has highlighted some corrosion damages that can affect geothermal equipment in contact with wet supercritical CO₂. At 110°C under 160 bar pressure, for equipment in contact with the sc CO₂ phase only a moderate uniform attack ($\approx 5 - 15 \mu\text{m}/\text{year}$) of the carbon steel and the AISI 410 stainless steel has been observed. For the samples immersed in the water phase, the salts dissolved in the water can greatly increase the rate of uniform corrosion of both carbon steels and AISI 410 stainless steel, from $100 \mu\text{m}/\text{year}$ for pure water to $300\text{-}500 \mu\text{m}/\text{year}$ when 50 g/L of NaCl is dissolved. The contamination with oxygen of the CO₂ has a dramatic effect on the corrosion of carbon steel and AISI 410 stainless steel in the water phase (≈ 3 to $5 \text{ mm}/\text{year}$). The passive layer of the ferritic AISI 410 stainless steel is destroyed and the lower grades of stainless steel are affected by localized corrosion such as crevices and pits.

REFERENCES

- Brown J., Graver B., Gulbrandsen E., Dugstad A., Morland B., Update of DNV Recommended Practice RP-J202 with Focus on CO₂ Corrosion with Impurities, *Energy Procedia*, 63 (2014) 2432–2441
- Cabrini M., Lorenzi S., Pastore T., Favilla M., Perini R. and Tarquini B. Materials selection for dew-point corrosion in geothermal fluids containing acid chloride, *Geothermics*, 69 (2017) 139–144
- Hua Y., Barker R., Charpentier T., Ward M., Neville A. (2015) Relating iron carbonate morphology to corrosion characteristics for water-saturated supercritical CO₂ systems, *The Journal of Supercritical Fluids*, 98 (2015) 183–193
- Kruszewski M. and Wittig V. Review of failure modes in supercritical geothermal drilling projects, *Geothermal Energy*, 6 (2018) 28
- Truesdell A. H., Haizlip J.R., Armannsson H. and D'Amore F. (1989) Origin and transport of chloride in superheated geothermal steam, *Geothermics*, 18 (1989) 295–30.
- Zhang Y., Gao K., Schmitt G. and Hausler R. H., Modeling steel corrosion under supercritical CO₂ conditions, *Materials and Corrosion*, 6 (2013) 478-485